THE JOURNAL OF PHYSICAL CHEMISTRY A

Feature Article

pubs.acs.org/JPCA

Dynamics of Chlorine Atom Reactions with Hydrocarbons: Insights from Imaging the Radical Product in Crossed Beams

Baptiste Joalland,[†] Yuanyuan Shi,[†] Armando D. Estillore,[†,§] Alexander Kamasah,[†] Alexander M. Mebel,[‡] and Arthur G. Suits*[,†]

[†]Department of Chemistry, Wayne State University, Detroit, Michigan 48202, United States

[‡]Department of Chemistry and Biochemistry, Florida International University, Miami, Florida 33199, United States

ABSTRACT: We present a comprehensive overview of our ongoing studies applying dc slice imaging in crossed molecular beams to probe the dynamics of chlorine atom reactions with polyatomic hydrocarbons. Our approach consists in measuring the full velocity-flux contour maps of the radical products using vacuum ultraviolet "soft" photoionization at 157 nm. Our overall goal is to extend the range of chemical dynamics investigations from simple triatomic or tetraatomic molecules to systematic investigations of a sequence of isomers or a homologous series of reactants of intermediate size. These experimental investigations are augmented by high-level ab initio calculations which, taken together, reveal trends in product energy and angular momentum partitioning and offer deep insight into the reaction mechanisms as a function of structure, bonding patterns, and kinematics. We explore these issues in alkanes, for which only direct reactive encounters are found, and in unsaturated hydrocarbons, for which an addition−elimination mechanism competes with direct abstraction. The results for alkene addition−elimination in particular suggest a new view of these reactions: The only pathway to HCl elimination is accessed by means of roaming excursions of the Cl atom from the strongly bound adduct.

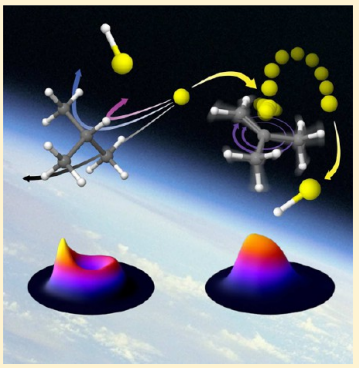

1. INTRODUCTION

Reactions of chlorine atoms with polyatomic hydrocarbons represent a vast body of important chemical events in atmospheric chemistry, notably as a source to form complex and highly reactive hydrocarbon radicals via metathesis reactions.[1,2] Chlorine atom is indeed a powerful oxidizing agent involved in some major environmental issues such as the ozone-destruction cycle,[3−5] the oxidation of volatile organic compounds in marine boundary layers[6,7] and Polar regions,[8,9] the burning of hazardous waste,[10,11] and possibly the aging of organic aerosols by heterogeneous processes.[12−14] Numerous kinetics studies have shown evidence of the high efficiency of hydrocarbon decomposition by Cl atoms.[15,16] These reactions are faster than those with the hydroxyl radical OH by at least 1 order of magnitude,[17] although OH is the primary daytime oxidant in the atmosphere. Interestingly, recent observations show evidence for an active chlorine chemistry in the interstellar medium, but its potential role in space has so far hardly been explored.[18,19] Studying Cl + RH reactions is also useful to gain a detailed understanding of combustion chemistry as exemplars of the free radical abstraction of hydrogen atoms in saturated hydrocarbons.[20,21] The high dimensionality and complexity of the potential energy surfaces (PESs), combined with experimental feasibility, are finally a central motivation to undertake detailed dynamics studies of Cl + RH reactions.[22−24]

Cl atom reactions with alkanes are prototypical direct H abstractions, with nearly no barrier from reactants to products. They lie in the intermediate regime; that is, these reactions are close to isoergicity. Considerable effort has been devoted to understanding the dynamics of this family of reactions, especially in the case of methane, CH_4, and its isotopologues.[25−30] Experimental outcomes with theoretical confirmation showed a cold vibrational and rotational state distribution in the nascent HCl/DCl (v′,j′) ascribed to a collinear C−H(D)−Cl transition state (TS), which turned out to be a universal signature of these reactions.[31−33] In contrast, reactions with alkenes leading to the formation of HCl are strongly exoergic, owing to the formation of resonantly stabilized radical products. Overall, the potential energy landscape is strongly affected by the presence of the CC double bond, with pronounced differences in reactive behavior for alkylic, allylic, or vinylic sites. The production of vibrationally excited HCl(v'=1) has been detected with 2,3-dimethylbut-2-ene in chlorinated solvents.[34] Furthermore, the dynamics of these reactions is considerably obscured by the competition between direct and indirect reactions. HCl + C_nH_{2n-1} products can indeed be formed via a Cl addition − HCl elimination mechanism involving a long-lived $C_nH_{2n}Cl$ intermediate.[35,36] The formation of HCl(v'=1) products has been attributed to direct reactions, whereas addition−elimination was assumed to give low vibrational excitation due to energy randomization in the long-lived adduct.[37] We will revisit this point in what follows.

Received: May 15, 2014
Revised: July 9, 2014

   dx.doi.org/10.1021/jp504804n | J. Phys. Chem. A XXXX, XXX, XXX−XXX

Fundamental achievements in the field of reaction dynamics were celebrated worldwide when in 1986, Herschbach,[38] Lee,[39] and Polanyi[40] shared the Nobel prize in Chemistry for their contributions on studying the dynamics of simple chemical reactions. Since these pioneering efforts, the emergence of ion imaging techniques[41] and their important enhancements have unraveled the dynamics of photochemical reactions and inelastic and reactive molecular collisions at an unprecedented level of detail.[42−44] The combination of crossed molecular beams with ion imaging allows for detection of any product mass and recoil energy combination without the kinematic constraints associated with measuring laboratory time-of-flight spectra. Furthermore, the center-of-mass distributions are simply a linear offset of the laboratory distributions, with no associated transformation Jacobian. The slice images themselves embody the velocity-flux contour maps that directly reflect the underlying collision dynamics. In other words, ion imaging turns the spotlight directly on the molecular forces acting at the moment of chemical reactions.

In this article, we wish to give a comprehensive overview on the dynamics of Cl atom reactions with a large collection of saturated and unsaturated C3 to C6 polyatomic hydrocarbons. We use a unique experimental setup based on the combination of crossed molecular beams and ion imaging techniques, with an emphasis on product radical detection.[45−52] Our approach is essentially equivalent to the 3D imaging technique used by Liu and co-workers to probe numerous methane reactions with radicals, among which are Cl atoms.[53,54] In these studies, vibrational level pair correlations obtained by probing the methyl radical product via resonance enhanced multiple photon ionization (REMPI) were exploited to gain new insight into the vibrational enhancement of the reaction cross section. We have also used REMPI to study the Cl + ethane reaction by state-selected HCl detection.[46] In the case of reactions involving larger systems, an alternative consists in probing the hydrocarbon radical product with vacuum ultraviolet (VUV) radiation. Several groups have performed single-photon ionization detection of polyatomic radicals produced in bimolecular reactions. Blank and Hemmi used tunable synchrotron radiation in the traditional crossed-beam configuration to study alkyl radicals formed in the reactions of Cl with propane and *n*-pentane.[55,56] The Davis group has pioneered the use of 157 nm radiation generated by an F_2 excimer laser to effect ionization of the products formed in metal−hydrocarbon bimolecular reactions,[57−59] and they are currently developing new soft and *unfocused* VUV photoionization techniques by nonlinear frequency conversion of table-top lasers.[60,61] In our laboratory we have used a 157 nm probe in reactive scattering experiments of $O(^3P)$ + alkane reactions,[62−64] $CN(X^2\Sigma^+)$ + alkene reactions,[65] and the forthcoming series of $Cl(^2P_{3/2})$ reactions.[47−52]

The article is structured as follows: section 2 highlights the experimental features of our crossed-beam dc slice imaging setup and the adopted protocol. Sections 3 and 4 present our experimental results on Cl reactions with alkanes and alkenes, respectively, along with ab initio calculations to characterize the potential energy surfaces (PESs). Section 5 gives an outlook of these results by focusing on the disentanglement between direct and indirect mechanisms and the role of roaming dynamics[66−68] in complex-mediated reactions. The discussion is given in section 6.

2. CROSSED-BEAM DC SLICE IMAGING

The experimental setup is given in Figure 1.[45,69] The machine is partitioned into two source chambers differentially evacuated to $\sim 10^{-7}$ Torr base and $\sim 10^{-5}$ Torr operational pressures by turbomolecular pumps, and a reaction chamber maintained permanently at $\sim 10^{-7}$ Torr or below to satisfy single-collision conditions. Molecular beams are supersonic expansions generated by piezoelectric valves pulsed at 10 Hz and skimmed upstream when entering in the main chamber. Hydrocarbons and precursors radicals are diluted in different inert gases (H_2/He/Ne/Ar, max. 5% of dilution percentage) to vary the collision energy. The scattered radical products are ionized with a F_2 excimer laser (157 nm, 7.9 eV) as soon as the products exit the interaction region. The ions are then accelerated via a four-electrode dc slice ion optics assembly to impact on a dual microchannel plate (MCP) detector coupled to a fast phosphor screen.[70] The front plate of the MCP assembly is held at constant potential, while the back plate "gates" the central slice of the reaction products at a specific m/z ratio by application of a high-voltage pulse. The resulting images are recorded using a charged-coupled device (CCD) camera, and the megapixel acquisition program IMACQ-2 is used to accumulate the raw images containing centroided data.[71] Background subtraction and density-to-flux corrections are performed prior to transforming the scattering distributions in the center-of-mass frame.

We have experimented with different radical sources to produce Cl atoms in their spin−orbit ground electronic state $^2P_{3/2}$. Compared to discharge sources, either in a single or a double stage configuration, we have preferred the use of photolysis of various precursors such as oxalyl chloride $(COCl)_2$,[72,73] tetrachloroethylene C_2Cl_4,[74] and the chlorine molecule Cl_2. $(COCl)_2$ and C_2Cl_4 precursors were dissociated with an ArF excimer laser producing 193 nm photons (10−20 mJ/pulse), and the third harmonic at 355 nm of a Nd:YAG

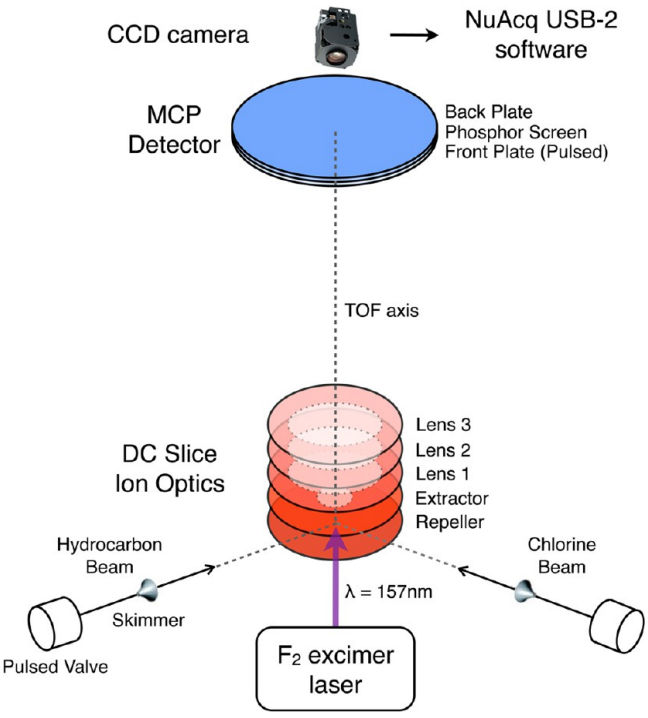

Figure 1. Schematic view of the crossed-beam apparatus combined with a universal dc slice imaging.

dx.doi.org/10.1021/jp504804n | J. Phys. Chem. A XXXX, XXX, XXX−XXX

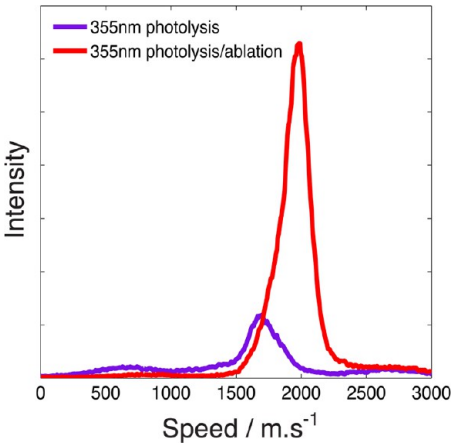

Figure 2. Chlorine beam profiles extracted from dc slice raw images recorded at $m/z = 35$ with and without ablation. Speed ratios are equal to 9 and 6, respectively. The effective Cl atom population reaching the interaction region is increased by a factor of 5 when ablation is used.

laser was used to dissociate Cl_2 (20 mJ/pulse). We have recently reported a high-density chlorine radical source.[51] For this purpose a cylindrical aluminum tube is attached to the end of the nozzle and confines the molecular beam along 5 cm with an inner diameter of 2 mm. A hole in the side of this extension tube allows us to focus the 355 nm laser beam at the tip of the nozzle. Compared to photolysis alone, the increase in the Cl beam profile intensity is significant, as shown in Figure 2 with a Cl atom population density enhanced by a factor of 5. Both the confinement of the free expansion and the aluminum laser ablation plume could induce, possibly together, this improvement. The scattering signals effectively measured after background subtraction were also significantly enhanced, thus permitting operational conditions with the VUV beam unfocused and a more selective detection with regard to the ionization energies (IEs) of the probed products (see section 3 for discussion on selectively deuterated alkanes). Only little density-to-flux correction was required.

3. CL + ALKANE REACTIONS

In this section we highlight our efforts in studying H abstraction processes by performing reactive scattering experiments with a large set of target systems such as propane and selectively deuterated isotopologues, and butane and pentane isomers for a large range of collision energies. The reaction enthalpies $\Delta_r H$ (0 K) are taken from ref 15 and the product IEs from the NIST webbook.[75]

3.1. Propane and Isotopologues. Propane is the smallest alkane exhibiting different and competing abstraction sites:

$$Cl(^2P) + CH_3CH_2CH_3 \rightarrow CH_3CH_2CH_2 + HCl \quad \Delta_r H(0\ K) = -2.0\ kcal{\cdot}mol^{-1} \quad (1)$$

$$Cl(^2P) + CH_3CH_2CH_3 \rightarrow CH_3CHCH_3 + HCl \quad \Delta_r H(0\ K) = -5.0\ kcal{\cdot}mol^{-1} \quad (2)$$

Partial deuteration only gives little changes in the global PESs (enthalpies of reaction $\Delta_r H(0\ K)$ are reduced by ~1 kcal·mol^{-1}), hence allowing for systematic studies to differentiate the dynamics of primary and secondary abstraction. Koplitz and

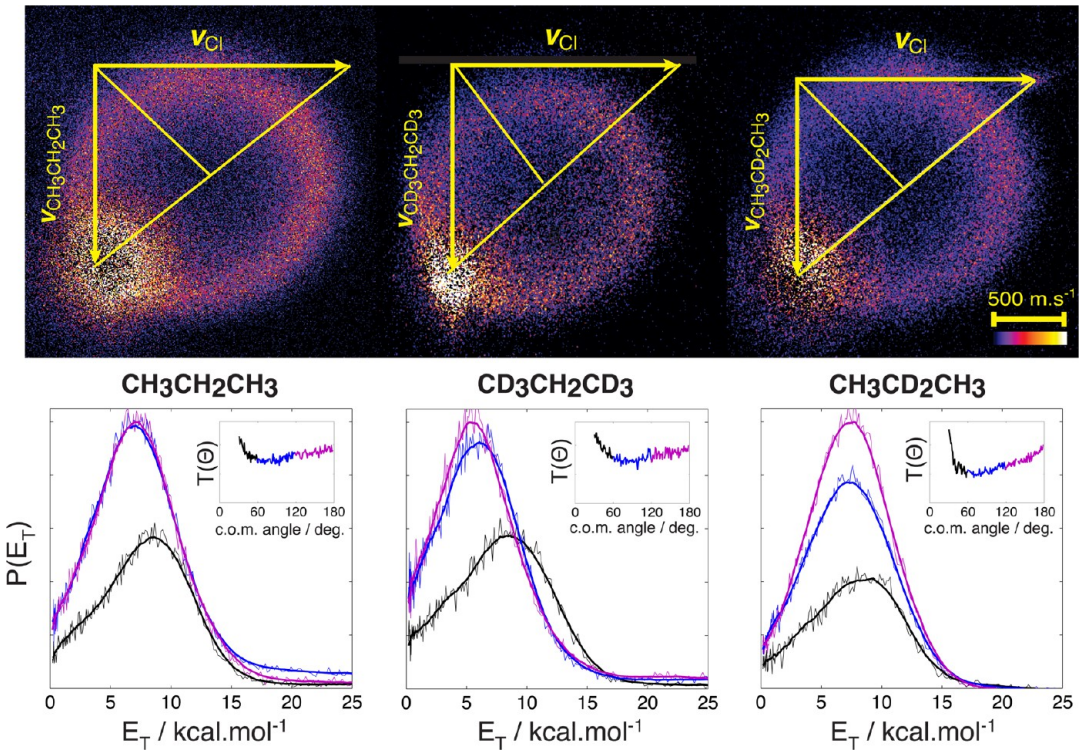

Figure 3. Direct current (dc) slice images and center-of-mass distributions of the radical products for the reaction of chlorine with propane and its two partially deuterated isotopologues at collision energies $E_C \sim 12$ kcal·mol^{-1}. Images are shown after background subtraction and density-to-flux correction and are superimposed with Newton diagrams. The scattering distributions are color-coded with the forward component in black (30−60°), the sideways component in blue (60−120°), and the backward component in purple (120−180°). The velocity-flux contour maps are shown with the photochemical background masked in the forward direction. Only reactions at the secondary abstraction sites are detected.

dx.doi.org/10.1021/jp504804n | J. Phys. Chem. A XXXX, XXX, XXX−XXX

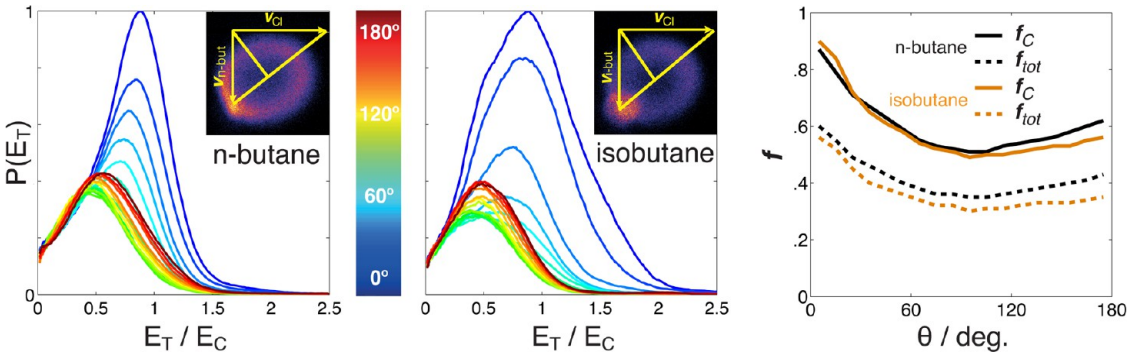

Figure 4. (Left) Reduced translational energy distributions of 10° steps measured for the reactions of chlorine with *n*-butane and isobutane at collision energies $E_C \sim 13$ kcal·mol^{-1}. The raw images and Newton diagrams are shown as insets. (Right) Fractions f_C and f_{tot} of collision energy E_C and available energy E_{tot}, respectively, appearing in translational energy E_T.

co-workers have reported that the secondary carbon is 3-fold more reactive than the primary ones on a per H atom basis by using a 2 + 1 REMPI detection of HCl/DCl.[76] With a similar detection scheme, Varley and Dagdigian measured sideways scattered DCl product while the HCl peaked in the backward direction in a photoloc[77,78] study of the Cl + $CD_3CH_2CD_3$ reaction.[32] Alternatively, Blank et al. used synchrotron radiation at ∼130 nm ($h\nu$ = 9.5 eV) to probe the propyl products formed in a crossed-beam apparatus. In this study the distributions in the scattering plane were determined by convolution fits from time-of-flight measurements at selected angles.[55]

Our results for the reactions of Cl atoms with $CH_3CH_2CH_3$, $CD_3CH_2CD_3$, and $CH_3CD_2CH_3$ were measured at $E_C \sim 12$ kcal·mol^{-1} and are shown in Figure 3. No primary abstraction products were detected, in line with a single-photon detection scheme that only ionizes the isopropyl products (IE = 7.7 eV) to the exclusion of *n*-propyl products (IE = 8.4 eV). The images, overlaid with Newton diagrams, show the recoil distributions after background subtraction and density-to-flux correction. The corresponding c.o.m. translational energy and angular distributions, respectively $P(E_T)$ and $T(\theta)$, are plotted. We distinguish the forward (FW, [30−60]°), the sideways (SW, [60−120]°), and the backward (BW, [120−180]°) directions. As we are probing the hydrocarbon radical in all these experiments, we refer to the hydrocarbon beam as the forward direction. The scattering regions in the [0−30]° range are truncated due to strong interferences with the photochemical background in the hydrocarbon target direction.

Overall, the three sets of translational energy and angular distributions show similar trends and are in excellent agreement with the results of Blank et al.[55] The translational energy of the FW scattering components peaks at ∼9 kcal·mol^{-1} whereas the SW/BW components peak at 5−7 kcal·mol^{-1}. The angular distribution exhibits a minimum in the [60−90]° range. A strong rise toward θ = 0° contrasts with a steady increase in the BW scattering region. Even truncated in the FW direction, these distributions are consistent with little interactions in the exit channel, as is inferred in general for these direct reactions and is consistent with the HCl rotational distributions. The FW translational energy is associated with a stripping mechanism for which only little reactant-to-product momentum transfers are expected, indicating weak interactions at the TS region and large impact parameters, while the effective partitioning of the available energy in the SW/BW suggests a rebound mechanism that favors the energy transfers into the internal degrees of freedom of the radical product. It should be noted that the SW/BW recoil of CD_3CHCD_3 is lower than that of the isopropyl products, although the data were collected at similar collision energies.

3.2. Butane Isomers. *n*-Butane is the simplest saturated hydrocarbon molecule that possesses different conformational minima. Primary and secondary abstractions show similar exoergicities to those of propane, while tertiary abstraction in isobutane is slightly more energetic:

$$\mathrm{Cl} + \mathrm{CH_3CH_2CH_2CH_3} \rightarrow \mathrm{CH_3CH_2CH_2CH_2} + \mathrm{HCl} \quad \Delta_r H(0\ \mathrm{K}) = -3.0\ \mathrm{kcal{\cdot}mol^{-1}} \tag{3}$$

$$\mathrm{Cl} + \mathrm{CH_3CH_2CH_2CH_3} \rightarrow \mathrm{CH_3CH_2CHCH_3} + \mathrm{HCl} \quad \Delta_r H(0\ \mathrm{K}) = -6.1\ \mathrm{kcal{\cdot}mol^{-1}} \tag{4}$$

$$\mathrm{Cl} + \mathrm{(CH_3)_3CH} \rightarrow \mathrm{(CH_3)_2CHCH_2} + \mathrm{HCl} \quad \Delta_r H(0\ \mathrm{K}) = -2.8\ \mathrm{kcal{\cdot}mol^{-1}} \tag{5}$$

$$\mathrm{Cl} + \mathrm{(CH_3)_3CH} \rightarrow \mathrm{(CH_3)_3C} + \mathrm{HCl} \quad \Delta_r H(0\ \mathrm{K}) = -8.1\ \mathrm{kcal{\cdot}mol^{-1}} \tag{6}$$

In the kinetics study by Sarzynski and Sztuba,[79] primary abstraction in n-C_4H_{10} showed a positive activation energy corresponding to a small barrier, while secondary abstraction was found to be barrierless. Varley and Dagdigian studied the Cl + $(CH_3)_3CD$ reaction and observed that the nascent DCl product was mainly backscattered, suggesting that abstraction of a tertiary hydrogen atom also proceeds via a near collinear transition state. Abstraction of the primary hydrogen to yield HCl was sideways peaked, in qualitative agreement with their results on primary abstraction with the Cl + $CH_3CD_2CH_3$ system. In the *photoloc* studies of Bass et al.,[80] abstraction of the primary H atom was reported to be FW scattered, while secondary abstraction was seen to be more isotropic. Toomes and Kitsopoulos[81] further studied the dynamics of Cl + butane by performing crossed beam imaging experiments in an unskimmed configuration. As in the reaction of Cl atom with smaller hydrocarbons, they reported the formation of rotationally cold HCl (v, j).[31] Both single-beam and crossed-beam studies, however, suffered from strong background interferences in the BW direction.

We have studied abstraction reactions with the two C_4H_{10} isomers in similar conditions as for the propane systems. The results were attributed to secondary abstraction in *n*-butane and tertiary abstraction in isobutane due to the product selectivity

dx.doi.org/10.1021/jp504804n | J. Phys. Chem. A XXXX, XXX, XXX−XXX

based on IEs. The experimental conditions allowed us to measure the whole scattering distributions at $E_C \sim 13$ kcal·mol^{-1}. $P(E_T)$ distributions are shown reduced by $E_T^* = E_T/E_C$ in Figure 4 to highlight the deviation from the kinematic picture of heavy-light-heavy reactive systems, for which the product translational energy will closely track the collision energy. We introduce the f_C factor, which is equal to the mean value of E_T^* averaged over a selected angle range and corresponds to the fraction of collision energy appearing in recoil. The f_{tot} factor corresponds to the fraction of available energy ($\Delta_r H(0\ K) + E_C$) appearing in recoil. Both f_C and f_{tot} are calculated each 10° in Figure 4. This illustrates well the two mechanisms in action with strong but parallel variations of energy transfer for both isomers: *n*-Butane and isobutane $P(E_T)$ peak near $f_C = 1$ at $\theta = 0°$, while large energy transfers with $f_C \sim 0.5$ are observed in the SW/BW directions. The similarities of f_C and f_{tot} along θ for both hydrocarbon targets support the idea that these direct reactions do not "see" the slight variations in exoergicity between the secondary and tertiary channels. However, the FW distribution of isobutane is more sharply peaked near $\theta = 0°$ and shows a broader translational energy release. The reasons for this are likely related to steric hindrance effects for this branched hydrocarbon.

The influence of collision energy on the differential cross sections of *n*-butane was measured for primary (D) and secondary (H) abstractions with the $CD_3CH_2CH_2CD_3$ system.[47] In this study, we used $(COCl)_2$ photolysis at 193 nm and a focused probe to study H and D abstractions at three collision energies, nearly 5, 10, and 13 kcal·mol^{-1}. As the collision energy increased, H and D distributions were both found to be dominated by a sharp FW scattered component, and the two isomer distributions are very similar at each collision energy. Overall, the scattering distributions of primary and secondary radicals showed remarkable similarities.

3.3. Pentane Isomers. H abstraction reactions were probed for three pentane isomers at two different collision energies: $E_C \sim 5$ and 9 kcal·mol^{-1},[47] with the probe laser focused at the interaction region. For *n*-pentane, the ratio of primary H atoms to secondary is 1:1, with enthalpies of reaction of −2.0 kcal·mol^{-1} and −5.3 kcal·mol^{-1}, respectively. For isopentane, a tertiary H with a reaction exothermicity of −8.2 kcal·mol^{-1} is present in addition to primary and secondary H atoms. Neopentane is the simplest hydrocarbon that possesses a quaternary carbon, and all the hydrogens are primary. The isomeric identity of the detected pentyl radical products is here not clear. For instance, abstraction of a primary H atom in *n*-pentane gives the 1-pentyl radical, while abstraction of a secondary H atom can give 2-pentyl or 3-pentyl radicals (IEs = 7.9, 7.1, 7.9 eV, respectively). The detection could therefore be substantially biased in favor of the 2-pentyl radicals. However, the relative ionization efficiency at 157 nm of the photoproducts of heptane isomers, among which are pentyl radicals, showed surprisingly little variation (less than 20%).[82] The results are therefore expected to be representative of the overall dynamics for all pentane isomers.

The scattering distributions, shown in Figure 5, are quite similar for all reactants. The translational energy distributions are strongly coupled to the angular distributions and show, for the FW scattered products, a sharp peak at $E_T^* \sim 0.8$ for all reactants at both collision energies. The SW scattered products show the lowest fraction of energy in translation, while the BW component peaks at the lowest energy ($E_T^* \sim 0.4$) but extends to the highest, showing evidence of coupling of the available

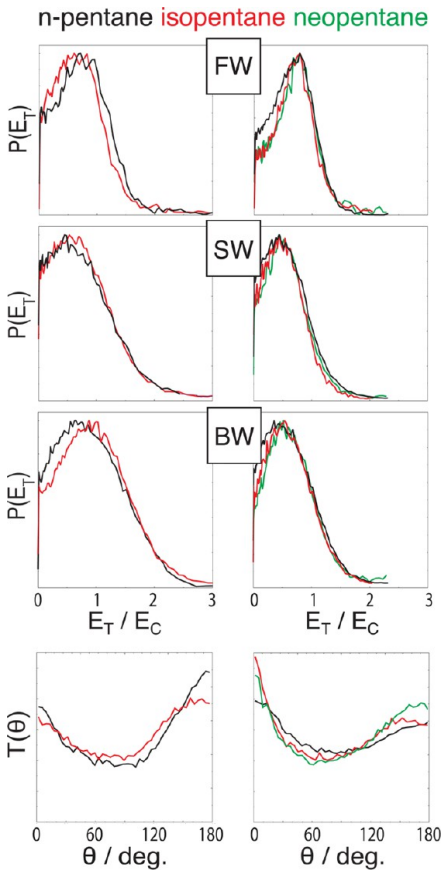

Figure 5. Reduced translational energy distributions and angular distributions for the reactions of chlorine with *n*-pentane (black), isopentane (red), and neopentane (green), at collision energies of 5 kcal·mol^{-1} (left) and 9 kcal·mol^{-1} (right).

energy into translation. The angular distributions show remarkable parallels for all systems. At lower collision energy there is a modest preference for BW scattering, and this shifts to sharp FW peaking for all cases at the higher collision energy. In agreement with the results obtained for propane and butanes, the nature of the abstraction site appears to have little influence on the dynamics under these conditions: The distinction between primary, secondary, and tertiary H abstraction is hardly visible in the dynamics of Cl + alkane reactions.

4. CL + ALKENE REACTIONS

Cl + alkene reactions are fast, with rate constants close to the gas kinetic limit.[16] Direct H abstraction producing HCl + C_nH_{2n-1} competes with Cl addition to the double bond to form $C_nH_{2n}Cl$ alkyl radicals, which may also decompose if the pressure is low enough, in order to release the excess energy gained in the addition step. Therefore, the rate constants are the combination of three distinct processes:

$$Cl + C_nH_{2n} + M \rightarrow C_nH_{2n}Cl^{\bullet} + M \quad (7)$$

$$Cl + C_nH_{2n} \rightarrow (C_nH_{2n}Cl)^* \rightarrow C_nH_{2n-1}^{\bullet} + HCl \quad (8)$$

$$Cl + C_nH_{2n} \rightarrow C_nH_{2n-1}^{\bullet} + HCl \quad (9)$$

The products of reactions 8 and 9 are identical on the basis of chemical formulas, although formation of distinct product isomers for these two pathways is possible. This class of

dx.doi.org/10.1021/jp504804n | J. Phys. Chem. A XXXX, XXX, XXX−XXX

Table 1. Enthalpies of Reactions $\Delta_r H$ at 0 K (kcal·mol^{-1}) for Cl Addition and HCl Elimination for the C4, C5, and C6 Alkenes Calculated at the CBS-QB3 Level of Theory, along with Vertical IEs of the Corresponding Products[a]

	Cl Addition		HCl Elimination								
			Allylic			Alkylic			Vinylic		
	Site	$\Delta_r H$	Site	$\Delta_r H$	IE	Site	$\Delta_r H$	IE	Site	$\Delta_r H$	IE
gauche-1-butene	C1	−20.6	C3	−20.8	7.6	C4	−2.9	8.5	C1	6.7	8.9
	C2	−20.8							C2	2.7	8.5
cis-2-butene	C2/C3	−22	C1/C4	−18.6	6.8				C2/C3	2.8	9.2
trans-2-butene	C2/C3	−22.3	C1/C4	−18.0	6.7				C2/C3	3.2	9.3
isobutene	C1	−22.1	C3/C4	−16.2	8.0				C1	7.3	8.8
	C2	−20.3									
1-pentene	C1	−21.0	C3	−20.3	7.5	C4	−5.9	6.8	C1	6.6	8.8
	C2	−20.6				C5	−3.1	7.5	C2	2.7	8.4
1-hexene	C1	−20.7	C3	−20.4	7.4	C4	−5.5	6.8	C1	6.6	8.9
	C2	−21.0				C5	−6.0	7.2	C2	2.8	8.4
						C6	−3.1	7.1			
2-hexene	C2	−22.0	C1	−17.9	7.4	C5	−5.9	6.3	C2	3.2	8.2
	C3	−22.9	C4	−20.5	7.0	C6	−3.2	7.6	C3	3.4	8.2

[a]See Figure 7 for carbon numeration in butene isomers.

reaction is indeed subject to multiple reaction mechanisms, owing to the presence of the CC double bond that induces strong variations in C−H bond strength and its associated reactivity for the removal of H atoms. To discriminate among these different pathways, several kinetic techniques have been developed; however, uncertainties on the exact mechanisms still persist due to the complexity of these systems.[16] Quantum chemical calculations also failed to corroborate the addition−elimination mechanism.[83,84]

Cl reactions were studied with four butene isomers, 1-pentene, 1-hexene, 2-hexene, and cyclohexene. The enthalpies of reactions were calculated at the CBS-QB3 level of theory to extrapolate the thermochemical data to the complete basis set (CBS) limit and provide a thermochemical accuracy of ∼2.0 kcal·mol^{-1}.[85−87] The values are presented in Table 1, along with the vertical IEs of the corresponding radical products. Complex formation is exothermic by ∼20 kcal·mol^{-1} for all systems, with a preference for the least substituted site (anti-Markovnikov behavior). We distinguish 3 types of HCl elimination sites: (i) the allylic sites, which are highly reactive with enthalpies of reaction in the [15−20] kcal·mol^{-1} range, (ii) the alkylic site, which is little affected by the double bond and exhibits enthalpies of reactions similar to those of primary and secondary abstractions in Cl + alkane reactions, and (iii) the vinylic sites, which are directly located at the double bond and are endoergic by [2−8] kcal·mol^{-1}.

4.1. Direct vs Indirect Mechanisms. We first investigated the reaction of chlorine atom with 1-pentene, 1-hexene, 2-hexene, and cyclohexene at two different collision energies: ∼4 and 7 kcal·mol^{-1}.[48] In this study, $(COCl)_2$ was used as a precursor and the probe laser was focused on the interaction region. The results are therefore representative of the overall dynamics with regard to the multiple sites accessible even at low collision energy. They are shown in Figure 6 with the $P(E_T)$ nonreduced to underline an important feature of these reactive systems: a considerable amount of available energy does not appear in the radical product recoil. This "missing" energy is therefore locked up in the internal energy of the products. With remarkable similarities over the different targets, a unique dynamical signature for this type of reaction appears, which contrasts with the direct H abstraction in alkanes: The

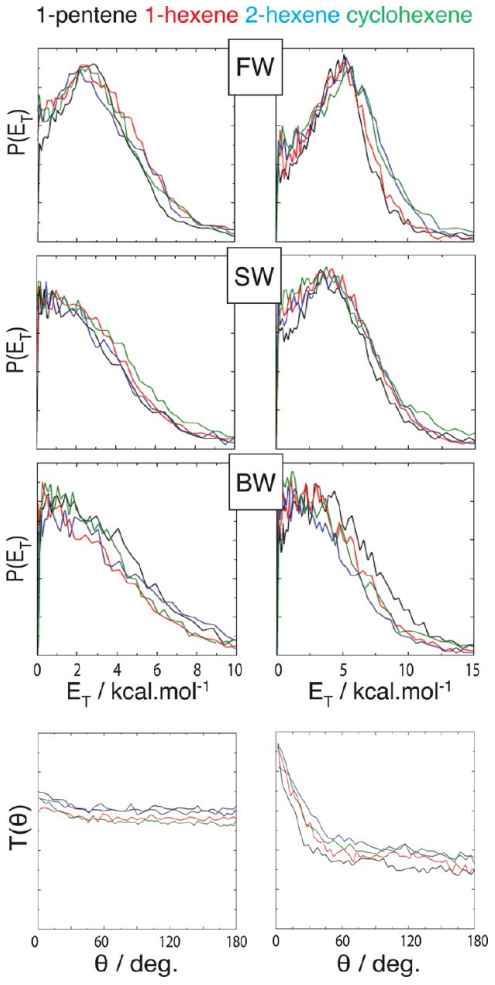

Figure 6. Translational energy distributions and angular distributions for the reactions of chlorine with 1-pentene (black), 1-hexene (red), 2-hexene (blue), and cyclohexene (green) at collision energies of 4 kcal·mol^{-1} (left) and 7 kcal·mol^{-1} (right).

angular distributions are found to be almost isotropic at low collision energy, suggesting reactions mediated by complex

dx.doi.org/10.1021/jp504804n | J. Phys. Chem. A XXXX, XXX, XXX−XXX

formation. At higher collision energy, the FW component is sharp and intense.

For a pure complex-forming reaction, a scattered distribution exhibiting FW/BW symmetry is expected. At low collision energy, the SW and BW distributions peak near zero recoil energy, while the FW direction shows a sharply peaked distribution. The FW component gains in intensity with increasing collision energy and begins to extend into the SW direction, whereas only subtle changes are observed in the BW distribution. There are two alternative ways to explain this behavior: The scattering distribution could lose forward−backward symmetry if the lifetime of the complex approaches its rotational period. This corresponds to the so-called "osculating complex" model of Herschbach.[88] Alternatively, a distinct component, superimposed on the isotropic component, grows in with increasing E_C. This latter argument is supported by the $P(E_T)$ translational energy distributions in the FW component. Similarly to reactions with alkanes, the FW distribution gains in intensity with increasing collision energy and begins to extend into the SW direction. The apparent absence of a direct component in the BW direction suggests that collisions at low impact parameters lead to complex formation prior to HCl release.

To get further insight into the dynamics of Cl + alkene reactions, we have measured scattering distributions for HCl elimination with a series of butene isomers, namely 1-butene, *cis*-2-butene, *trans*-2-butene, and isobutene (2-methylpropene) for $E_C \sim 13$ kcal·mol^{-1}.[52] The photolysis/ablation chlorine atom source and the soft photoionization scheme were used to probe the various C_4H_7 butenyl products. The velocity-flux contour maps and Newton diagrams are shown in Figure 7 along with reduced $P(E_T)$ and $T(\theta)$. These results are obtained at much higher collision energies than the previous results on C5−C6 alkenes but are more selective with regard to IEs. All potential alkylic and vinylic radicals exhibit IEs higher than 8.5 eV, to be compared to the one of *n*-propyl (8.4 eV), for which no scattering signal was detected in the reactions with partially deuterated propane. In contrast, all the IEs of allylic radicals lie below 8.0 eV, with the latter corresponding to the isobutenyl radical, for which a value of 7.9 eV was measured experimentally.[89]

The 1-butene reduced translational distribution peaks at $E_T^* = 0.5$ in the SW/BW direction and 0.8 in the FW direction. These peak values match well the average recoil with $f_C \sim 0.5$ and 0.7 in the SW/BW and FW directions, respectively. For all the other isomers, the three angular components show similar average recoil with a f_C factor near 0.5. 1-Butene possesses two conformers, *cis* and *gauche*, that exhibit similar energetics, but we consider only the gauche conformer according to IR strong-field results obtained for similar free-jet adiabatic expansion.[90] This system has the shallowest well and the most exoergic abstraction channel, in line with the slightly higher recoil of the FW scattered products. On the other hand, isobutene has both the deepest well for addition at the C1 site and the lowest exoergicity for HCl elimination; the scattering distribution is here more FW/BW symmetric and the average recoil slightly lowered. On the basis of these trends, the distributions for Cl reactions with C_4H_8 isomers seem to reflect the energetics of the competition between direct and indirect mechanisms.

The isobutene system is an excellent alkene target to rule out any possible reactions at sites other than the allylic ones: Propene has a unique allylic site and induces more important photochemical interferences in the FW direction, while the

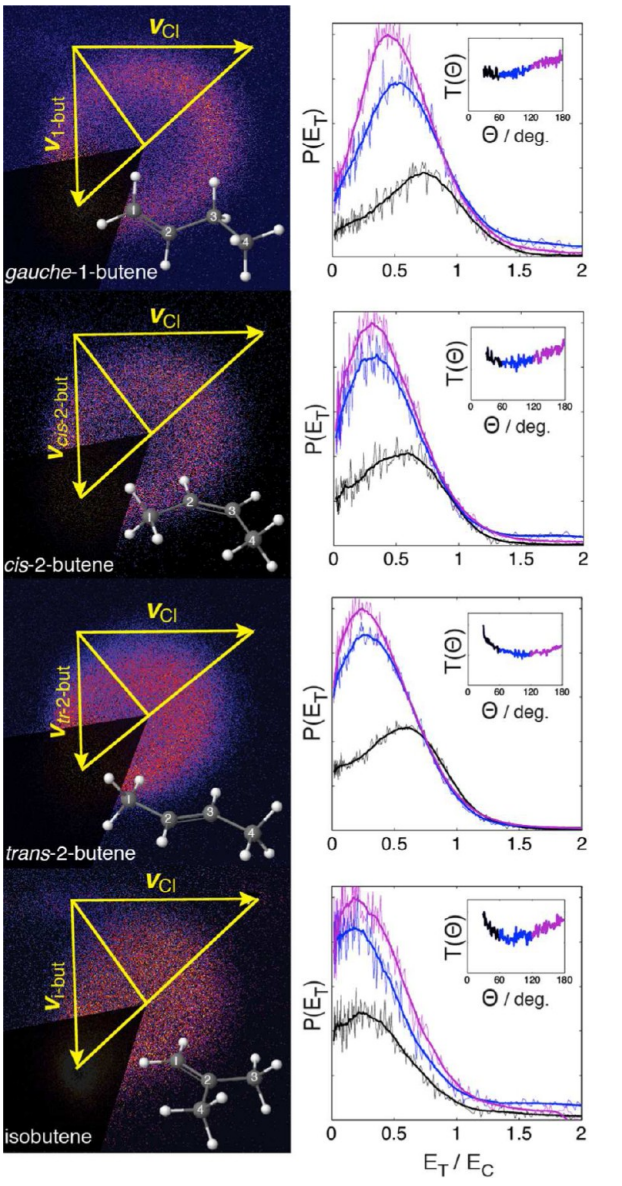

Figure 7. Direct current (dc) slice images and reduced center-of-mass distributions for the reactions of chlorine with 1-butene, *cis*-2-butene, *trans*-2-butene, and isobutene at collision energies of ∼12 kcal·mol^{-1}. The forward component is represented in black (30−60°), sideways in blue (60−120°), and backward in purple (120−180°).

enhanced complexity of the PESs of larger systems may blur the attacked site differentiation. Reaction at the vinylic sites of isobutene is the most endoergic among the here studied alkenes, with $\Delta_r H(0\ K) = 7.3$ kcal·mol^{-1}, and no alkylic site is present. Because the scattering distribution of isobutyl suggests complex-mediated reaction, we now look into more detail of the dynamics of this system by varying the collision energy. The results are shown in Figure 8. For $E_C = 14$ kcal·mol^{-1}, the distributions look quite similar to those of saturated species. Two distinct FW and SW/BW components are seen in the $P(E_T)$ with a higher recoil in the FW direction. $T(\theta)$ shows a minimum around $\theta = 90°$. At 8 kcal·mol^{-1}, the product translational energy diminishes in every direction, and the direct BW component seems to vanish, in agreement with previous results on C5−C6 alkenes at similar collision energies. The average recoil is located near $f_C = 0.8$, to be compared to

dx.doi.org/10.1021/jp504804n | J. Phys. Chem. A XXXX, XXX, XXX−XXX

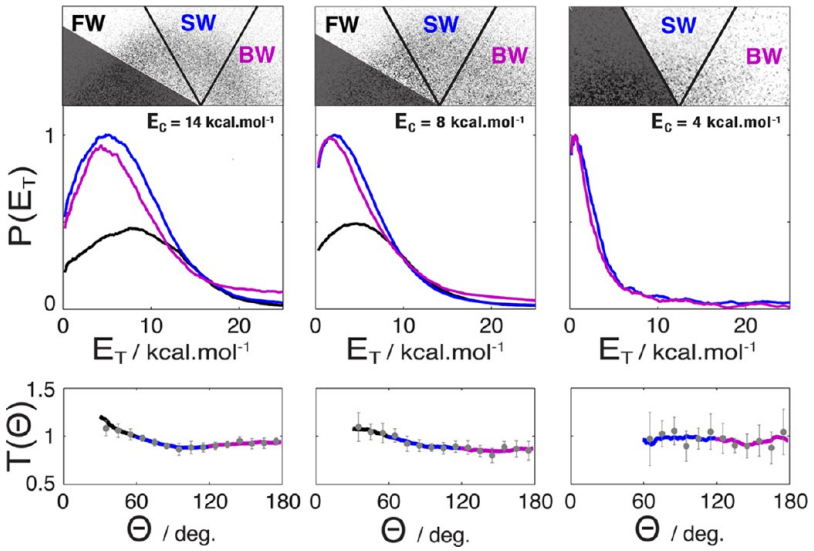

Figure 8. Center-of-mass distributions of the isobutenyl C_4H_7 radical for different collision energies. Translational energy distributions $P(E_T)$ and angular distributions $T(\theta)$ are plotted for forward (30−60°, black), sideways (60−120°, blue), and backward (120−180°, purple) scattered products. The velocity−flux contour maps are shown with the photochemical background masked in the forward direction. Error bars were estimated each 10° via single standard deviation.

0.6 at E_C = 14 kcal·mol^{-1}. Both values are compatible with the trends observed for direct abstractions in Cl + alkane reactions. At 4 kcal·mol^{-1}, the C_4H_7 recoil peaks near zero and the angular distribution is isotropic. Only 10% of the available energy appears in translation, and f_C drops down to nearly 0.4. This low product recoil reflects an effective randomization of the internal energy over the vibrational degrees of freedom in the long-lived adduct prior to HCl release. In these indirect reactions, the system loses reference to the initial approach direction. As a consequence, the FW/BW symmetry is manifested by a fully isotropic distribution.

4.2. Roaming in Addition−Elimination Reactions. These observations raise the question of the nature of the possible transition state(s) for addition−elimination reactions. The key stationary points for the Cl + isobutene reaction, calculated at the CBS-QB3 level of theory, are shown in Figure 9A. Direct H abstraction is exoergic by 16.2 kcal·mol^{-1} at the allylic sites and endoergic by 7.3 kcal·mol^{-1} at the vinylic site. The Cl approaches isobutene without any barrier to form a C_4H_7...HCl van der Waals complex, which is bound by 2.6 kcal·mol^{-1} with respect to the C_4H_7 + HCl products. The absence of barriers was confirmed via a careful scan of the minimal energy reaction path through partial geometry optimization, with the critical H−Cl and C−H distances being frozen for the entrance channel and the exit channel, respectively. For reaction at the vinylic site, no transition state has been located. The Cl addition onto C1 or C2 carbons is also barrierless and leads to the formation of $H_2CClC(CH_3)_2$ and $H_2CCCl(CH_3)_2$ radicals, respectively, which reside in deep potential wells of 20−22 kcal·mol^{-1}. No tight transition states for HCl elimination were located from these complexes. Nevertheless, we were able to find pathways connecting these strongly bound C_4H_8Cl intermediates with the allylic C_4H_7 + HCl channel. The structure of the TS along the addition−elimination pathway is highlighted in Figure 9A. The Cl−H distance for forming the H−Cl bond is 2.39 Å, with the corresponding attacked C−H bond stretched only to 1.11 Å. The Cl atom is 3.47 and 3.94 Å away from the C2 and C1 carbons, respectively. Intrinsic reaction coordinate (IRC) calculations show that the TS is connected to the van der Waals $H_2CCCH_3CH_2$...HCl product complex. In the reverse direction, IRC calculations return back to the C2 addition complex. However, since the Cl atom is located far from both C1 and C2, the downhill pathway from the TS can also bifurcate to the C1 addition complex, as seen in Figure 9B. This is a typical TS for a roaming radical mechanism,[66] in which the Cl atom unlinks from the CC double bond, is about to be eliminated (returning to reactants), but wanders in the direction of the allylic site and picks up a hydrogen from a methyl group to form HCl.

We have performed similar calculations for Cl reaction with all other butene isomers. Only roaming-type transition states for addition−elimination were found, although the PESs were complicated by additional H abstraction sites. The pathways from the adducts to the products involve no conventional 3-center or 4-center transition states which are located 1−2 kcal·mol^{-1} below the reactant asymptotes. While roaming dynamics are now widely recognized as an important pathway in unimolecular reactions,[66−68] we show here that they are central to the Cl addition−HCl elimination mechanism: Even though abstraction is the only pathway to products, an indirect reaction can occur mediated by the strong electrophilic interaction of the Cl atom with the alkene π cloud.

Preliminary results based on statistical dissociation rate constants calculated in the Rice−Ramsperger−Kassel−Marcus framework[91] show that the lifetimes of the Cl-complexes upon dissociation, estimated from energy-dependent rate constant calculations, are too long at both low and high energies (72 and 2 ns, respectively) to account for the onset of the forward component observed in the isobutene scattering distributions when compared to the rotational period (~30 ps) of the complex. This observation further rules out a possible "osculating complex" responsible for breaking FW/BW symmetry in the observed scattered products.

5. DISCUSSION

Two distinct mechanisms associated with direct H/D abstractions, stripping and rebound, are clearly identified in the scattered alkyl product distributions of Cl + alkane

dx.doi.org/10.1021/jp504804n | J. Phys. Chem. A XXXX, XXX, XXX−XXX

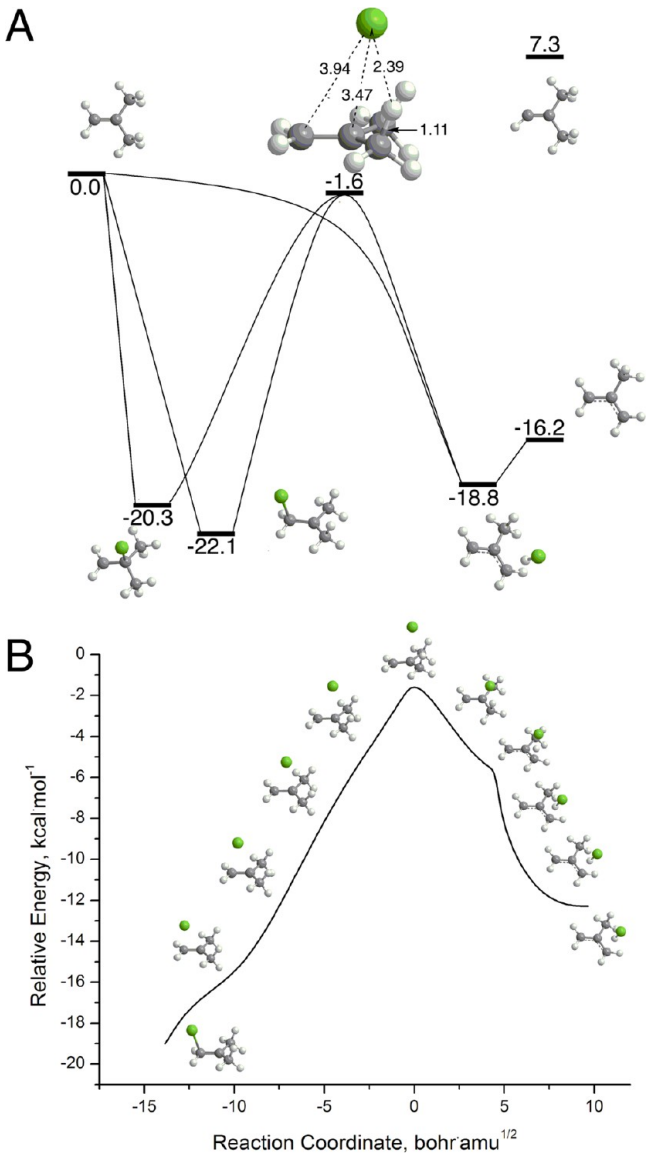

Figure 9. (A) Key points on the potential energy surface of the Cl + isobutene reaction. Direct H abstraction is a barrierless pathway with a van der Waals complex in the exit channel. The two addition complexes undergo near dissociation to reach a unique roaming-type transition state (TS-C3 roam) before eliminating HCl. The diagram has been calculated at the CBS-QB3 level of theory. Relative energies are shown in kcal·mol^{-1}. (B) Minimal energy profile and structures along the $ClCH_2C(CH_3)_2 \rightarrow CH_2C(CH_3)(CH_2)$...HCl pathway via the roaming transition state, extracted from IRC calculations at the B3LYP/6-311G(2d,d,p) level.

reactions. Our results show in a consistent manner the importance of the backscattered distributions at all collision energies, thus shedding light on the most closely coupled dynamics, that is the rebound mechanism. Compared to previous state-selected HCl experiments in both *photoloc*[80] and crossed-beam[81] studies, there is here no photochemical background in the SW/BW scattering directions by probing the radical products. We found no characteristic dynamical features for primary, secondary, or tertiary abstractions could be unambiguously extracted from these results. However, distinct dynamical behaviors were observed for butane isomers in the FW directions, suggesting that, even if stripping is barely sensitive to the energetics of the reaction, this mechanism can be affected by steric hindrance. Most notably, our experimental investigations reveal an important trend in the product recoil of these reactions involving large hydrocarbons: the recoil velocity of the SW/BW components decreases with increasing size of the alkane reactant.

To get further insight in these trends and deviations from smaller systems, we first invoke a simple kinematic model suggested by Evans et al.,[92] in which the average translational energy release is given by

$$E_T = E_C \cos^2 \beta + E_R \sin^2 \beta$$

where β is the skew angle for the reaction, E_C is the collision energy, and E_R is the energy release in the reaction. The skew angle is defined for $A + BC$ by $\cos^2 \beta = (m_A m_B)/(m_{AB} m_{BC})$ and embodies key kinematics for the reaction. In this linear triatomic model, the remaining energy is allocated to vibrational excitation of the newly formed HCl bond. This picture therefore provides a rough limiting view to account for relaxation of the alkyl radical from the TS geometry. Here, the skew angle is acute, as typically seen in heavy−light−heavy hydrogen transfer reactions, so the first term strongly dominates. Our measurements show that, in all cases, the observed translational energy releases of the BW scattered products are lower than the predicted value from this model whatever the collision energy. For the reaction of O(^{3}P) + butane, Liu et al. observed a similar trend and concluded that 4−5 kcal·mol^{-1} was not available for the product alkyl recoil.[63] Large polyatomic systems such as those studied here possess several repositories for the excess energies, in particular vibrations or rotations of the alkyl radical product. A simple hybrid Franck−Condon/impulsive model has been developed to account for the rotational excitation E_{rot} of the alkyl radical product in the F + ethane reaction:[93]

$$E_{rot} = L^2/2I = Mb^2 \sin^2 \theta E_T$$

where L is the angular momentum, I and M the moment of inertia and the mass of the alkyl radical, respectively, and b and θ the impact parameter and the torque angle, respectively. However, this model refers to a reaction picture with a deep exit channel that favors the energy transfers into the degrees of rotation of the products, so it is less suitable for Cl + alkane reactions. If we compare the propane distributions to each other and to the butane isomers, the average recoil of the products diminishes while the size/density-of-state increases, and opposite to the trend expected if radical rotation is the principal repository of the energy, therefore ruling out this model and further suggesting the importance of vibrational excitation of the alkyl radicals in this case. New investigations with quantum scattering calculations[94,95] or quasi-classical trajectories[96−98] seem to be the only alternative to reveal the subtleties of energy disposal in Cl + alkane reactions.

To put into perspective our results and highlight the differences between Cl + alkanes and Cl + alkenes reactions, we plot in Figure 10 all the f_C factors measured for the different systems, along with those for Cl reactions with butanol isomers. The latter show strong similarities with the alkane ones, in agreement with the HCl(v'=0) rotational distributions measured by Rudić and co-workers.[99,100] For alkanes/alcohols, the translational energy release is close to 1 at low collision energy, and it diminishes to values of ∼0.6 at higher collision energies, showing again evidence for an effective partitioning of the available energy into product translation. The results with

dx.doi.org/10.1021/jp504804n | J. Phys. Chem. A XXXX, XXX, XXX−XXX

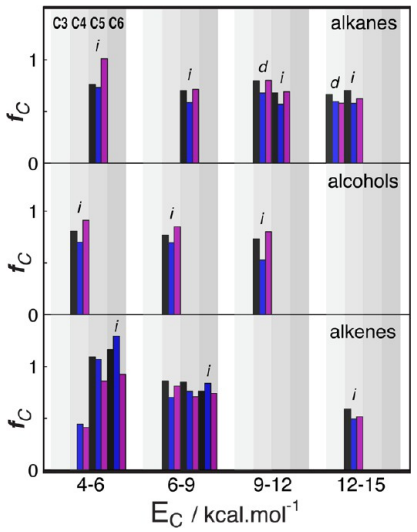

Figure 10. Fractions f_C of collision energy appearing in the radical product recoil for the different sizes of alkanes, alcohols, and alkenes studied with universal dc slice imaging. FW is colored in black, SW in blue, and BW in purple. Values are averaged with deuterated species (d) and isomers (i) when specified.

alkenes exhibit much greater variations, in terms of both size and collision energies. In particular, the differences between isobutene, 1-pentene, and hexenes are somewhat striking at low collision energy, while at high collision energy the "missing" energy is more pronounced than that for alkanes/alcohols. At low E_C, the large C5−C6 systems show the only f_C values above 1 for this collection of results, illustrating the coupling of the exoergicity into translation. The isobutenyl recoil is way below at $f_C \sim 0.4$. This contrasts with Cl + alkane results that show a strong coupling of product recoil and exoergicity at low collision energies. One must invoke both the energetics and the reaction mechanisms to explain these large variations in energy recoil. In isobutene, only reactions at the allylic sites (C3/C4, 6 H atoms) are accessible at E_C = 4 kcal·mol^{-1}, while for the C5−C6 distributions the reaction competes with direct H abstraction at the alkylic sites. The latter reactions show similar exoergicities with primary and secondary abstractions in Cl + alkane reactions (~3 and 6 kcal·mol^{-1}, respectively), and they are accessible to the VUV probe based on product IEs. Moreover, reactions at the vinylic site, albeit unlikely, cannot strictly be ruled out. As a consequence, these important variations are likely to be due to the detection of both addition−elimination at the allylic sites and direct abstraction at the alkylic sites for the C5−C6 alkene distributions, while isobutene data are consistent with a large contribution of addition−elimination.

The Cl + isoprene reaction was studied earlier theoretically by Braña and Sordo,[83] who were looking for the addition−elimination pathway in order to explain the pressure dependence of the reaction rate constant observed in kinetics experiments. However, the authors have not found any conventional three- or four-center transition states for HCl elimination from the addition complex and attributed the observed pressure dependence to the existence of a weakly bound C_5H_7...HCl product complex. We show in Figure 11 the PES of the Cl + isoprene reaction also calculated at the CBS-QB3 level of theory. The picture appears to be similar to the one for butene isomers: We confirm there is no "conventional", tight transition state for HCl elimination at the allylic site from the various possible adducts, but only TSs of roaming character connecting the adducts to the formation of HCl at the unique allylic sites. Although we were not able to observe any reactive scattering signal corresponding to the HCl elimination, the formation of the adduct was seen for the first time in our crossed-beam dc slice imaging apparatus. This observation is consistent with the dissociation rate constants of Cl−isoprene complexes calculated in the RRKM framework: They indeed appear to be significantly slower compared to those of Cl−butene complexes, with lifetimes equal to 6.0 μs, 0.8 μs, and 86 ns, at E_C = 4, 8, and 14 kcal·mol^{-1}. Therefore, we believe that the addition−elimination reactions mediated by the roaming

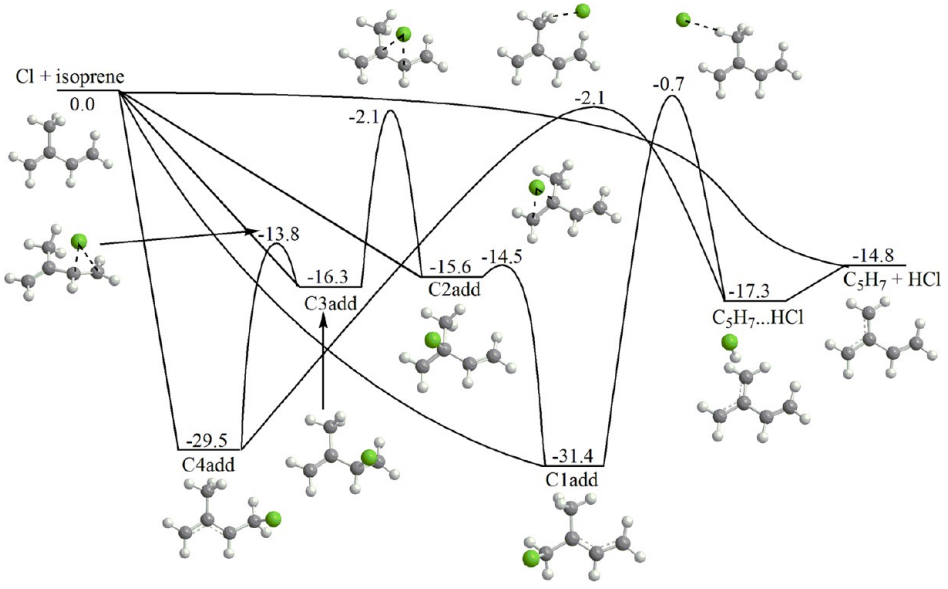

Figure 11. Key points on the potential energy surface of the Cl + isoprene reaction. Direct H abstraction at the unique allylic site and Cl additions are barrierless. Two roaming TSs are found: one following C4 addition and the other following C1 addition. The diagram has been calculated at the CBS-QB3 level of theory. Relative energies are shown in kcal·mol^{-1}.

dx.doi.org/10.1021/jp504804n | J. Phys. Chem. A XXXX, XXX, XXX−XXX

radical mechanism are also effective here, but the long lifetimes of the corresponding adducts do not allow us to probe their decomposition before they leave the interaction region of the crossed molecular beams.

Finally, a clear distinction between roaming-mediated addition−elimination and direct reactions that simply avoid the deep well of the adduct or deviate from the minimum energy path must be emphasized. Here, the roaming dynamics represent an important subset of these reactions: it is analogous to the roaming component in the H + HCO reaction,[101] except there is no other route to products from the adduct. The HCl molecules formed in this case could also be vibrationally excited owing to the loose character of the TS and the large reaction exoergicity. Recent work in the Orr-Ewing group on isobutene and other related species has shown by direct dynamics simulations the importance of such Cl excursions in the long-range interaction before H abstraction can occur.[102] As a consequence, the HCl product vibrational distributions may not be useful to distinguish between direct and indirect reaction pathways. The other important consequence of this is on the expected kinetic isotope effects. The addition step would be characterized by an inverse KIE (a higher density-of-states in the deuterated molecule stabilizes the adduct compared to the undeuterated molecule), while the roaming-abstraction step would show a normal KIE owing to the difference in zero point energies. It is not clear how these opposing effects would appear in the effective KIE. This offers a very distinctive view of radical addition/elimination in alkenes: The π cloud captures the radical and retains it until it finds the right approach to the abstraction geometry in which reaction can occur, allowing transfer of excess energy to internal degrees of freedom of the hydrocarbon and thereby prolonging the interaction time. The roaming mechanism, involving near dissociation back to reactants, is not simply an aspect of these dynamics, it is at their very heart.

6. CONCLUSION

In this work we take advantage of probing the radical products with a VUV soft ionization detection scheme implemented in a crossed-beam slice imaging setup to reveal trends in product energy and angular momentum partitioning of chlorine atoms reactions with a series of C3−C6 alkanes and alkenes. The sensitivity of our approach allows us to show strong and subtle variations in the scattered distributions measured at varying collision energies. In Cl + alkanes reactions, the product distributions are consistent with direct H abstractions. For these reactions no clear signatures for primary, secondary, or tertiary H abstraction are observed. However, the variations in the recoil of the backward component associated with the rebound mechanism suggest that the vibrational excitation of the radical product plays an important role. This dynamical picture contrasts both with Cl reactions with smaller alkanes and with F + alkanes reactions. We also show that the products stemming from the stripping mechanism in branched alkanes can experience steric effects that broaden their angular distributions. In Cl + alkene reactions, the overall dynamics is profoundly modified by the presence of the CC double bound. We show in particular the significant role played by complex-mediated addition−elimination reactions at low collision energies. These results are augmented with high-level ab initio calculations. A selection of alkene targets and a careful scan of the potential energy surfaces demonstrate that HCl elimination from C_4H_8Cl intermediates can occur exclusively via a Cl roaming radical mechanism. In these indirect reactions, the strongly bound adduct experiences near dissociation due to its high internal energies, but it finds a pathway in the long-range interaction region to eliminate HCl instead of returning back to the reactants. Our results also suggest a significant weight of complex-mediated reactions in the total reaction cross sections at higher collision energies. We are currently investigating the reaction rate constants of these reactions by variational transition-state theory and are continuing our crossed-beam dc slice imaging studies. We plan to extend our studies to OH reactions, although those reactions are far more challenging due to the considerably lower reaction rate constants compared to those of Cl atom reactions.

AUTHOR INFORMATION

Corresponding Author

*E-mail: asuits@wayne.edu.

Present Address

[§](A.E.) Department of Chemistry, University of California, Berkeley, CA 94720.

Notes

The authors declare no competing financial interest.

Biographies

Baptiste Joalland received a Masters degree in Physics at University Paris-XI and a Ph.D. in Astrochemistry at University of Toulouse, France. He was a visiting scientist at the Institute of Physics in Rennes prior to joining Arthur G. Suits laboratory at Wayne State University as a postdoctoral fellow.

Yuanyuan Shi received a Bachelors degree in Chemistry from University of Science and Technology of China (2011) and then started to pursue her Ph.D. degree at Wayne State University and joined A. G. Suits Lab in 2011.

dx.doi.org/10.1021/jp504804n | J. Phys. Chem. A XXXX, XXX, XXX−XXX

Armando D. Estillore obtained his B.S. degree in Chemistry from Iligan Institute of Technology of the Mindanao State University, Philippines. He then went on to study reaction dynamics using crossed-beam ion imaging at Wayne State University in the group of Prof. Arthur G. Suits, receiving his Ph.D. in 2012. Currently, he is the Camille and Henry Dreyfus Postdoctoral Fellow in Environmental Chemistry at the University of California—Berkeley in the group of Prof. Kristie A. Boering.

Alexander Kamasah received his Bachelor's degree in chemistry from the University of Cape-Coast in Ghana and then proceeded to East Tennessee State University for his Master's degree in chemistry in the year 2011. He then began his Ph.D. program at Wayne State University and joined A.G Suits lab in 2012.

Alexander M. Mebel received his bachelor's degree in physical chemistry at the Moscow Institute of Steel and Alloys and his Ph.D. degree in physical chemistry at Kurnakov's Institute of General and Inorganic Chemistry of Russian Academy of Science in Moscow, Russia. After postdoctoral appointments in Germany, Japan, and USA, his first faculty position was at the Institute of Atomic and Molecular Sciences (Academia Sinica, Taiwan), and in 2003 he joined the Department of Chemistry and Biochemistry of Florida International University in Miami, Florida, USA, where he is currently Professor of Chemistry.

Arthur G. Suits received his B.S. in Chemistry from the University of Missouri, Columbia, in 1986 and his Ph.D. from the University of California, Berkeley, in 1991. Following a postdoctoral appointment at Cornell University, he held staff positions at Lawrence Berkeley National Laboratory and Brookhaven National Laboratory and on the Faculty of Stony Brook University before joining the Chemistry Department at Wayne State University as Professor of Chemistry in 2004. He is a Fellow of the APS and the AAAS and currently holds an A. Paul Schaap Senior Faculty Fellowship at Wayne State and a Radboud Excellence Professorship at Radboud University, Nijmegen.

■ ACKNOWLEDGMENTS

This research was supported by the Director, Office of Science, Office of Basic Energy Science, Division of Chemical Science, Geoscience and Bioscience, of the U.S. Department of Energy under Contracts No. DE-FG02-04ER15593 (to A.G.S., Wayne State University) and DE-FG01-04ER15570 (to A.M.M., Florida International University). A.G.S. also acknowledges an A. Paul Schaap Senior Faculty Fellowship at Wayne State University. We thank Laura M. Visger-Kiefer, Tarek Abdul Ghani, Richard Van Camp, and Nitin Patel for their contributions in the work presented herein.

■ REFERENCES

(1) Finlayson-Pitts, B. J.; Pitts, J. N. Tropospheric Air Pollution: Ozone, Airborne Toxics, Polycyclic Aromatic Hydrocarbons, and Particles. *Science* **1997**, *276* (5315), 1045−1051.

(2) Atkinson, R.; Arey, J. Gas-Phase Tropospheric Chemistry of Biogenic Volatile Organic Compounds: A Review. *Atmos. Environ.* **2003**, *37*, 197−219.

(3) Molina, M. J.; Rowland, F. S. Stratospheric Sink for Chlorofluoromethanes: Chlorine Atom-Catalysed Destruction of Ozone. *Nature* **1974**, *249* (5460), 810−12.

(4) Solberg, S.; Schmidbauer, N.; Semb, A.; Stordal, F.; Hov, Ø. Boundary-Layer Ozone Depletion as Seen in the Norwegian Arctic in Spring. *J. Atmos. Chem.* **1996**, *23* (3), 301−332.

(5) Platt, U.; Hönninger, G. The Role of Halogen Species in the Troposphere. *Chemosphere* **2003**, *52* (2), 325−338.

(6) Wingenter, O. W.; Kubo, M. K.; Blake, N. J.; Smith, T. W.; Blake, D. R.; Rowland, F. S. Hydrocarbon and Halocarbon Measurements as Photochemical and Dynamical Indicators of Atmospheric Hydroxyl, Atomic Chlorine, and Vertical Mixing Obtained During Lagrangian Flights. *J. Geophys. Res.—Atmos.* **1996**, *101* (D2), 4331−4340.

(7) Lawler, M. J.; Finley, B. D.; Keene, W. C.; Pszenny, A. A. P.; Read, K. A.; Von Glasow, R.; Saltzman, E. S. Pollution-Enhanced

Reactive Chlorine Chemistry in the Eastern Tropical Atlantic Boundary Layer. *Geophys. Res. Lett.* **2009**, *36*, 8.
(8) Jobson, B. T.; Niki, H.; Yokouchi, Y.; Bottenheim, J.; Hopper, F.; Leaitch, R. Measurements of C2-C6 Hydrocarbons During the Polar Sunrise 1992 Experiment: Evidence for Cl Atom and Br Atom chemistry. *J. Geophys. Res.—Atmos.* **1994**, *99* (D12), 25355−25368.
(9) Ariya, P. A.; Jobson, B. T.; Sander, R.; Niki, H.; Harris, G. W.; Hopper, J. F.; Anlauf, K. G. Measurements of C2-C7 Hydrocarbons During the Polar Sunrise Experiment 1994: Further Evidence for Halogen Chemistry in the Troposphere. *J. Geophys. Res.—Atmos.* **1998**, *103* (D11), 13169−13180.
(10) Hitchman, M. L.; Spackman, R. A.; Ross, N. C.; Agra, C. Disposal Methods for Chlorinated Aromatic Waste. *Chem. Soc. Rev.* **1995**, *24* (6), 423−430.
(11) Zimmermann, R.; Blumenstock, M.; Heger, H. J.; Schramm, K.-W.; Kettrup, A. Emission of Nonchlorinated and Chlorinated Aromatics in the Flue Gas of Incineration Plants During and After Transient Disturbances of Combustion Conditions: Delayed Emission Effects. *Environ. Sci. Technol.* **2001**, *35* (6), 1019−1030.
(12) George, I. J.; Abbatt, J. P. D. Heterogeneous Oxidation of Atmospheric Aerosol Particles by Gas-Phase Radicals. *Nat. Chem.* **2010**, *2* (9), 713−722.
(13) Liu, C.-L.; Smith, J. D.; Che, D. L.; Ahmed, M.; Leone, S. R.; Wilson, K. R. The Direct Observation of Secondary Radical Chain Chemistry in the Heterogeneous Reaction of Chlorine Atoms with Submicron Squalane Droplets. *Phys. Chem. Chem. Phys.* **2011**, *13* (19), 8993−9007.
(14) Mendez, M.; Ciuraru, R.; Gosselin, S.; Batut, S.; Visez, N.; Petitprez, D. Reactivity of Chlorine Radical with Submicron Palmitic Acid Particles: Kinetic Measurements and Product Identification. *Atmos. Chem. Phys.* **2013**, *13* (23), 11661−11673.
(15) Atkinson, R. Gas-Phase Tropospheric Chemistry of Volatile Organic Compounds: 1. Alkanes and Alkenes. *J. Phys. Chem. Ref. Data* **1997**, *26* (2), 215−290.
(16) Taatjes, C. A. Time-Resolved Infrared Absorption Measurements of Product Formation in Cl Atom Reactions with Alkenes and Alkynes. *Int. Rev. Phys. Chem.* **1999**, *18*, 419.
(17) Spicer, C. W.; Chapman, E. G.; Finlayson-Pitts, B. J.; Plastridge, R. A.; Hubbe, J. M.; Fast, J. D.; Berkowitz, C. M. Unexpectedly High Concentrations of Molecular Chlorine in Coastal Air. *Nature* **1998**, *394* (6691), 353−356.
(18) Neufeld, D. A.; Roueff, E.; Snell, R. L.; Lis, D.; Benz, A. O.; Bruderer, S.; Black, J. H.; De Luca, M.; Gerin, M.; Goldsmith, P. F. Herschel Observations of Interstellar Chloronium. *Astrophys. J.* **2012**, *748* (1), 37.
(19) Monje, R. R.; Lis, D. C.; Roueff, E.; Gerin, M.; De Luca, M.; Neufeld, D. A.; Godard, B.; Phillips, T. G. Hydrogen Chloride in Diffuse Interstellar Clouds Along the Line of Sight to W31C (G10. 6−0.4). *Astrophys. J.* **2013**, *767* (1), 81.
(20) DeSain, J. D.; Klippenstein, S. J.; Taatjes, C. A.; Hurley, M. D.; Wallington, T. J. Product Formation in the Cl-Initiated Oxidation of Cyclopropane. *J. Phys. Chem. A* **2003**, *107* (12), 1992−2002.
(21) Glarborg, P. Hidden Interactions—Trace Species Governing Combustion and Emissions. *Proc. Combust. Inst.* **2007**, *31* (1), 77−98.
(22) Liu, K. Crossed-Beam Studies of Neutral Reactions: State-Specific Differential Cross Sections. *Annu. Rev. Phys. Chem.* **2001**, *52* (1), 139−164.
(23) Murray, C.; Orr-Ewing, A. J. The Dynamics of Chlorine-Atom Reactions with Polyatomic Organic Molecules. *Int. Rev. Phys. Chem.* **2004**, *23*, 435.
(24) Bechtel, H. A.; Camden, J. P.; Brown, D. J.; Martin, M. R.; Zare, R. N.; Vodopyanov, K. Effects of Bending Excitation on the Reaction of Chlorine Atoms with Methane. *Angew. Chem., Int. Ed. Engl.* **2005**, *117* (16), 2434−2437.
(25) Simpson, W. R.; Orr-Ewing, A. J.; Zare, R. N. State-to-State Differential Cross-Sections for the Reaction $Cl(^2P_{3/2})$ + $CH_4(\nu_3=1,J=1) \rightarrow HCl(v'=1,J') + CH_3$. *Chem. Phys. Lett.* **1993**, *212*, 163.
(26) Simpson, W. R.; Rakitzis, T. P.; Kandel, S. A.; Orr-Ewing, A. J.; Zare, R. N. Reaction of Cl with Vibrationally Excited CH_4 and CHD_3—State-to-State Differential Cross-Sections and Steric Effects for the HCl Product. *J. Chem. Phys.* **1995**, *103*, 7313.
(27) Simpson, W. R.; Orr-Ewing, A. J.; Rakitzis, T. P.; Kandel, S. A.; Zare, R. N. Core Extraction for Measuring State-to-State Differential Cross-Sections of Bimolecular Reactions. *J. Chem. Phys.* **1995**, *103*, 7299.
(28) Simpson, W. R.; Rakitzis, T. P.; Kandel, S. A.; Lev-On, T.; Zare, R. N. Picturing the Transition-State Region and Understanding Vibrational Enhancement for the Cl + $CH_4 \rightarrow$ HCl + CH_3 Reaction. *J. Phys. Chem.* **1996**, *100*, 7938.
(29) Orr-Ewing, A. J.; Simpson, W. R.; Rakitzis, T. P.; Kandel, S. A.; Zare, R. N. Scattering-angle resolved product rotational alignment for the reaction of Cl with vibrationally excited methane. *J. Chem. Phys.* **1997**, *106*, 5961.
(30) Zhou, J.; Lin, J. J.; Zhang, B.; Liu, K. On the $Cl^*(^2P_{1/2})$ Reactivity and the Effect of Bend Excitation in the Cl + CH_4/CD_4 Reactions. *J. Phys. Chem. A* **2004**, *108* (39), 7832−7836.
(31) Varley, D. F.; Dagdigian, P. J. Product State Distributions and Angular Differential Cross Sections from Photoinitiated Reactions of Chlorine Atoms with Small Hydrocarbons. *J. Phys. Chem.* **1995**, *99* (24), 9843−9853.
(32) Varley, D. F.; Dagdigian, P. J. Comparison of the Dynamics of Abstraction of Primacy vs Secondary Hydrogens in the Cl + $CD_3CH_2CD_3$ Reaction. *Chem. Phys. Lett.* **1996**, *255*, 393.
(33) Varley, D. F.; Dagdigian, P. J. Product State Resolved Study of the Cl + $(CH_3)_3CD$ Reaction: Comparison of the Dynamics of Abstraction of Primary versus Tertiary Hydrogens. *J. Phys. Chem.* **1996**, *100* (11), 4365−4374.
(34) Abou-Chahine, F.; Greaves, S. J.; Dunning, G. T.; Orr-Ewing, A. J.; Greetham, G. M.; Clark, I. P.; Towrie, M. Vibrationally Resolved Dynamics of the Reaction of Cl Atoms with 2,3-Dimethylbut-2-ene in Chlorinated Solvents. *Chem. Sci.* **2013**, *4* (1), 226−237.
(35) Ragains, M. L.; Finlayson-Pitts, B. J. Kinetics and mechanism of the reaction of Cl atoms with 2-methyl-1,3-butadiene (isoprene) at 298 K. *J. Phys. Chem. A* **1997**, *101*, 1509.
(36) Kaiser, E. W.; Wallington, T. J. Pressure Dependence of the Reaction Cl + C_3H_6. *J. Phys. Chem.* **1996**, *100*, 9788.
(37) Arunan, E.; Rengarajan, R.; Setser, D. W. Infrared Chemiluminescence Studies of the Reactions of H Atoms with CCl_3, CF_2Cl, and CH_2CH_2Cl Radicals at 300 and 475 K: Recombination-Elimination vs. Abstraction Mechanisms. *Can. J. Chem.* **1994**, *72*, 568.
(38) Herschbach, D. R. Molecular Dynamics of Elementary Chemical Reactions. *Angew. Chem., Int. Ed. Engl.* **1987**, *26*, 1221−1243.
(39) Lee, Y. T. Molecular Beam Studies of Elementary Chemical Processes. *Science* **1987**, *236*, 793−798.
(40) Polanyi, J. C. Some Concepts in Reaction Dynamics. *Science* **1987**, *236*, 680−690.
(41) Chandler, D. W.; Houston, P. L. Two-Dimensional Imaging of State-Selected Photodissociation Products Detected by Multiphoton Ionization. *J. Chem. Phys.* **1987**, *87*, 1445−1447.
(42) Heck, A. J. R.; Chandler, D. W. Imaging Techniques for the Study of Chemical Reaction Dynamics. *Annu. Rev. Phys. Chem.* **1995**, *46* (1), 335−372.
(43) Ashfold, M. N. R.; Nahler, N. H.; Orr-Ewing, A. J.; Vieuxmaire, O. P. J.; Toomes, R. L.; Kitsopoulos, T. N.; Garcia, I. A.; Chestakov, D. A.; Wu, S.-M.; Parker, D. H. Imaging the dynamics of gas phase reactions. *Phys. Chem. Chem. Phys.* **2006**, *8* (1), 26−53.
(44) Suits, A. G.; Continetti, R. E. *Imaging in chemical dynamics*; American Chemical Society Publications: 2001; Vol. *770*.
(45) Ahmed, M.; Peterka, D. S.; Suits, A. G. Imaging H Abstraction Dynamics in Crossed Molecular Beams: Cl + ROH Reactions. *Phys. Chem. Chem. Phys.* **2000**, *2*, 861.
(46) Li, W.; Huang, C. S.; Patel, M.; Wilson, D.; Suits, A. State-Resolved Reactive Scattering by Slice Imaging: A New View of the Cl + C_2H_6 Reaction. *J. Chem. Phys.* **2006**, *124*, 11102.

(47) Estillore, A. D.; Visger, L. M.; Suits, A. G. Crossed-Beam DC Slice Imaging of Chlorine Atom Reactions with Pentane Isomers. *J. Chem. Phys.* **2010**, *132*, 164313.
(48) Estillore, A. D.; Visger, L. M.; Suits, A. G. Imaging the Dynamics of Chlorine Atom Reactions with Alkenes. *J. Chem. Phys.* **2010**, *133*, 074306.
(49) Estillore, A. D.; Visger-Kiefer, L. M.; Ghani, T. A.; Suits, A. G. Dynamics of H and D Abstraction in the Reaction of Cl Atom with Butane-1,1,1,4,4,4-d6. *Phys. Chem. Chem. Phys.* **2011**, *13* (18), 8433−8440.
(50) Estillore, A. D.; Visger-Kiefer, L. M.; Suits, A. G. Reaction Dynamics of Cl + Butanol Isomers by Crossed-Beam Sliced Ion Imaging. *Faraday Discuss.* **2012**, *157*, 181−191.
(51) Joalland, B.; Shi, Y.; Patel, N.; Van Camp, R.; Suits, A. G. Dynamics of Cl + Propane, Butanes Revisited: A Crossed Beam Slice Imaging Study. *Phys. Chem. Chem. Phys.* **2013**.
(52) Joalland, B.; Shi, Y.; Akamasah, A.; Suits, A. G.; Mebel, A. M. Roaming Dynamics in Radical Addition-Elimination Reactions. *Nat. Commun.* **2014**, *5*, 4064.
(53) Yan, S.; Wu, Y.-T.; Zhang, B.; Yue, X.-F.; Liu, K. Do Vibrational Excitations of CHD_3 Preferentially Promote Reactivity toward the Chlorine Atom? *Science* **2007**, *316* (5832), 1723−1726.
(54) Wang, F.; Lin, J.-S.; Cheng, Y.; Liu, K. Vibrational Enhancement Factor of the Cl + CHD_3 (v_1 = 1) Reaction: Rotational-Probe Effects. *J. Phys. Chem. Lett.* **2013**, *4* (2), 323−327.
(55) Blank, D. A.; Hemmi, N.; Suits, A. G.; Lee, Y. T. A Crossed Molecular Beam Investigation of the Reaction Cl + Propane → HCl + C_3H_7 Using VUV Synchrotron Radiation as a Product Probe. *Chem. Phys.* **1998**, *231*, 261.
(56) Hemmi, N.; Suits, A. G. The Dynamics of Hydrogen Abstraction Reactions: Crossed-Beam Reaction Cl + n-C_5H_{12} → C_5H_{11} + HCl. *J. Chem. Phys.* **1998**, *109*, 5338.
(57) Stauffer, H. U.; Hinrichs, R. Z.; Willis, P. A.; Davis, H. F. Competing reaction pathways from Y + C[sub 2]H[sub 2] collisions. *J. Chem. Phys.* **1999**, *111* (9), 4101−4112.
(58) Willis, P. A.; Stauffer, H. U.; Hinrichs, R. Z.; Davis, H. F. Rotatable Source Crossed Molecular Beams Apparatus with Pulsed Ultraviolet/Vacuum Ultraviolet Photoionization Detection. *Rev. Sci. Instrum.* **1999**, *70*, 2606.
(59) Willis, P. A.; Stauffer, H. U.; Hinrichs, R. Z.; Davis, H. F. Crossed beams study of C-H bond activation: Mo([sup 5]S[sub 2]) + CH[sub 4] –> MoCH[sub 2] + H[sub 2]. *J. Chem. Phys.* **1998**, *108* (7), 2665−2668.
(60) Albert, D. R.; Proctor, D. L.; Davis, H. F. High-Intensity Coherent Vacuum Ultraviolet Source Using Unfocussed Commercial Dye Lasers. *Rev. Sci. Instrum.* **2013**, *84* (6), 063104.
(61) Albert, D. R.; Davis, H. F. Studies of Bimolecular Reaction Dynamics Using Pulsed High-Intensity Vacuum-Ultraviolet Lasers for Photoionization Detection. *Phys. Chem. Chem. Phys.* **2013**, *15* (35), 14566−14580.
(62) Gross, R. L.; Liu, X. H.; Suits, A. G. O(^{3}P) versus O(^{1}D) Reaction Dynamics with n-Pentane: A Crossed-Beam Imaging Study. *Chem. Phys. Lett.* **2003**, *376*, 710.
(63) Liu, X.; Gross, R. L.; Hall, G. E.; Muckerman, J. T.; Suits, A. G. Imaging O(^{3}P) + Alkane Reactions in Crossed Molecular Beams: Vertical versus Adiabatic H Abstraction Dynamics. *J. Chem. Phys.* **2002**, *117* (17), 7947−7959.
(64) Liu, X.; Gross, R. L.; Suits, A. G. Differential Cross-Sections for O(^{3}P) + Alkane Reactions by Direct Imaging. *J. Chem. Phys.* **2002**, *116* (13), 5341−5344.
(65) Estillore, A. D.; Visger, L. M.; Kaiser, R. I.; Suits, A. G. Crossed-Beam Imaging of the H Abstraction Channel in the Reaction of CN with 1-Pentene. *J. Phys. Chem. Lett.* **2010**, *1*, 2417−2421.
(66) Townsend, D.; Lahankar, S. A.; Lee, S. K.; Chambreau, S. D.; Suits, A. G.; Zhang, X.; Rheinecker, J.; Harding, L. B.; Bowman, J. M. The Roaming Atom: Straying from the Reaction Path in Formaldehyde Decomposition. *Science* **2004**, *306* (5699), 1158−1161.
(67) Suits, A. G. Roaming Atoms and Radicals: A New Mechanism in Molecular Dissociation. *Acc. Chem. Res.* **2008**, *41* (7), 873−881.
(68) Bowman, J. M.; Shepler, B. C. Roaming Radicals. *Annu. Rev. Phys. Chem.* **2011**, *62*, 531−553.
(69) Huang, C. S.; Li, W.; Suits, A. G. Rotationally Resolved Reactive Scattering: Imaging Detailed Cl + C_2H_6 Reaction Dynamics. *J. Chem. Phys.* **2006**, *125*, 133107.
(70) Townsend, D.; Minitti, M. P.; Suits, A. G. Direct Current Slice Imaging. *Rev. Sci. Instrum.* **2003**, *74*, 2530.
(71) Li, W.; Chambreau, S. D.; Lahankar, S. A.; Suits, A. G. Megapixel ion imaging with standard video. *Rev. Sci. Instrum.* **2005**, *76*, 63106.
(72) Ahmed, M.; Blunt, D.; Chen, D.; Suits, A. G. UV Photodissociation of Oxalyl Chloride Yields Four Fragments from One Photon Absorption. *J. Chem. Phys.* **1997**, *106*, 7617.
(73) Hemmi, N.; Suits, A. G. Photodissociation of Oxalyl Chloride at 193 nm Probed via Synchrotron Radiation. *J. Phys. Chem. A* **1997**, *101*, 6633.
(74) Herath, N.; Hause, M. L.; Suits, A. G. The Photodissociation Dynamics of Tetrachloroethylene. *J. Chem. Phys.* **2011**, *134* (16), 164301−7.
(75) NIST webbook (webbook.nist.gov/chemistry).
(76) Yen, Y. F.; Wang, Z.; Xue, B.; Koplitz, B. Site Propensities for Hydrogen Chloride and Deuterium Chloride Formation in the Reaction of Chlorine Atom with Selectively-Deuterated Propanes. *J. Phys. Chem.* **1994**, *98* (1), 4−7.
(77) Aoiz, F. J.; Brouard, M.; Enriquez, P. A.; Sayos, R. Analysis of Product Doppler-Broadened Profiles Generated from Photoinitiated Bimolecular Reactions. *J. Chem. Soc., Faraday Trans.* **1993**, *89* (10), 1427−1434.
(78) Shafer, N. E.; Orr-Ewing, A. J.; Simpson, W. R.; Xu, H.; Zare, R. N. State-to-State Differential Cross-Sections from Photoinitiated Bulb Reactions. *Chem. Phys. Lett.* **1993**, *212* (1), 155−162.
(79) Sarzynski, D.; Sztuba, B. Gas-Phase Reactions of Cl Atoms with Propane, n-Butane, and Isobutane. *Int. J. Chem. Kinet.* **2002**, *34* (12), 651−658.
(80) Bass, M. J.; Brouard, M.; Vallance, C.; Kitsopoulos, T. N.; Samartzis, P. C.; Toomes, R. L. The Dynamics of the Cl + n-C_4H_{10} → HCl (v',j') + C_4H_9 Reaction at 0.32 eV. *J. Chem. Phys.* **2004**, *121*, 7175.
(81) Toomes, R. L.; Kitsopoulos, T. N. Rotationally-Resolved Reaction Product Imaging Using Crossed Molecular Beams. *Phys. Chem. Chem. Phys.* **2003**, *5*, 2481.
(82) Silva, R.; Gichuhi, W. K.; Doyle, M. B.; Winney, A. H.; Suits, A. G. Photodissociation of Heptane Isomers and Relative Ionization Efficiencies of Butyl and Propyl Radicals at 157 nm. *Phys. Chem. Chem. Phys.* **2009**, *11*, 4777.
(83) Braña, P.; Sordo, J. A. Mechanistic Aspects of the Abstraction of an Allylic Hydrogen in the Chlorine Atom Reaction with 2-Methyl-1,3-butadiene (Isoprene). *J. Am. Chem. Soc.* **2001**, *123* (42), 10348−10353.
(84) Braña, P.; Sordo, J. A. Theoretical Approach to the Mechanism of Reactions between Halogen Atoms and Unsaturated Hydrocarbons: The Cl + Propene Reaction. *J. Comput. Chem.* **2003**, *24* (16), 2044−2062.
(85) Montgomery, J. A.; Frisch, M. J.; Ochterski, J. W.; Petersson, G. A. A Complete Basis Set Model Chemistry. VI. Use of Density Functional Geometries and Frequencies. *J. Chem. Phys.* **1999**, *110*, 2822.
(86) Montgomery, J. A.; Frisch, M. J.; Ochterski, J. W.; Petersson, G. A. A Complete Basis Set Model Chemistry. VII. Use of the Minimum Population Localization Method. *J. Chem. Phys.* **2000**, *112*, 6532.
(87) Frisch, M. J.; Trucks, G. W.; Schlegel, H. B.; Scuseria, G. E.; Robb, M. A.; Cheeseman, J. R.; Scalmani, G.; Barone, V.; Mennucci, B.; Petersson, G. A.; Nakatsuji, H.; Caricato, M.; Li, X.; Hratchian, H. P.; Izmaylov, A. F.; Bloino, J.; Zheng, G.; Sonnenberg, J. L.; Hada, M.; Ehara, M.; Toyota, K.; Fukuda, R.; Hasegawa, J.; Ishida, M.; Nakajima, T.; Honda, Y.; Kitao, O.; Nakai, H.; Vreven, T.; Montgomery, J. A. J.; Peralta, J. E.; Ogliaro, F.; Bearpark, M.; Heyd, J. J.; Brothers, E.; Kudin, K. N.; Staroverov, V. N.; Kobayashi, R.; Normand, J.; Raghavachari, K.; Rendell, A.; Burant, J. C.; Iyengar, S. S.; Tomasi, J.; Cossi, M.; Rega,

N.; Millam, J. M.; Klene, M.; Knox, J. E.; Cross, J. B.; Bakken, V.; Adamo, C.; Jaramillo, J.; Gomperts, R.; Stratmann, R. E.; Yazyev, O.; Austin, A. J.; Cammi, R.; Pomelli, C.; Ochterski, J. W.; Martin, R. L.; Morokuma, K.; Zakrzewski, V. G.; Voth, G. A.; Salvador, P.; Dannenberg, J. J.; Dapprich, S.; Daniels, A. D.; Farkas, O.; Foresman, J. B.; ; Ortiz, J. V.; Cioslowski, J.; Fox, D. J. *Gaussian 09, Revision A.02*; Gaussian, Inc.: Wallington, CT, 2009.

(88) Fisk, G. A.; McDonald, J. D.; Herschbach, D. R. General discussion. *Discuss. Faraday Soc.* **1967**, *44*, 228.

(89) Schultz, J. C.; Houle, F. A.; Beauchamp, J. L. Photoelectron Spectroscopy of Isomeric C_4H_7 Radicals. Implications for the Thermochemistry and Structures of the Radicals and Their Corresponding Carbonium Ions. *J. Am. Chem. Soc.* **1984**, *106* (24), 7336−7347.

(90) Kunitski, M.; Knippenberg, S.; Dreuw, A.; Brutschy, B. The Conformational Stability of Gaseous 1-Butene Studied by Femtosecond Nonlinear Spectroscopy and *ab initio* calculations. *Vib. Spectrosc.* **2011**, *56* (1), 13−18.

(91) Fernández-Ramos, A.; Miller, J. A.; Klippenstein, S. J.; Truhlar, D. G. Modeling the Kinetics of Bimolecular Reactions. *Chem. Rev.* **2006**, *106* (11), 4518−4584.

(92) Evans, G. T.; van Kleef, E.; Stolte, S. Chemical Reaction Dynamics: Combination of Two Models. *J. Chem. Phys.* **1990**, *93* (7), 4874−4883.

(93) Whitney, E. S.; Zolot, A. M.; McCoy, A. B.; Francisco, J. S.; Nesbitt, D. J. Reactive Scattering Dynamics in Atom + Polyatomic Systems: F + C_2H_6 → HF (v',J') + C_2H_5. *J. Chem. Phys.* **2005**, *122* (12), 124310.

(94) Althorpe, S. C.; Clary, D. C. Quantum Scattering Calculations on Chemical Reactions. *Annu. Rev. Phys. Chem.* **2003**, *54* (1), 493−529.

(95) Shan, X.; Clary, D. C. Quantum Effects in the Abstraction Reaction by H Atoms of Primary and Secondary Hydrogens in n-C_4H_{10}: A Test of a New Potential Energy Surface Construction Method. *Phys. Chem. Chem. Phys.* **2013**, *15* (4), 1222−1231.

(96) Persky, A.; Broida, M. Quasiclassical Trajectory Study of the Reaction O(^{3}P) + HCl → OH + Cl. The Effects of Vibrational Excitation, Rotational Excitation, and Isotopic Substitution on the Dynamics. *J. Chem. Phys.* **1984**, *81* (10), 4352−4362.

(97) Bonnet, L.; Rayez, J.-C. Quasiclassical Trajectory Method for Molecular Scattering Processes: Necessity of a Weighted Binning Approach. *Chem. Phys. Lett.* **1997**, *277* (1), 183−190.

(98) Sathyamurthy, N.; Raff, L. Quasiclassical Trajectory Studies Using 3D Spline Interpolation of Ab Initio Surfaces. *J. Chem. Phys.* **2008**, *63* (1), 464−473.

(99) Rudić, S.; Ascenzi, D.; Orr-Ewing, A. J. Rotational Distribution of the HCl Products from the Reaction of Cl(^{2}P) Atoms with Methanol. *Chem. Phys. Lett.* **2000**, *332* (5), 487−495.

(100) Rudić, S.; Murray, C.; Ascenzi, D.; Anderson, H.; Harvey, J. N.; Orr-Ewing, A. J. The Dynamics of Formation of HCl Products from the Reaction of Cl Atoms with Methanol, Ethanol, and Dimethyl Ether. *J. Chem. Phys.* **2002**, *117*, 5692.

(101) Christoffel, K. M.; Bowman, J. M. Three Reaction Pathways in the H + HCO → H_2 + CO Reaction. *J. Phys. Chem. A* **2009**, *113* (16), 4138−4144.

(102) Preston, T. J.; Dunning, G. T.; Orr-Ewing, A. J.; Vázquez, S. A. Direct and Indirect Hydrogen Abstraction in Cl + Alkene Reactions. *J. Phys. Chem. A* **2014**, DOI: 10.1021/jp5042734.